RESPONSE: The authors appreciate the thoughtful and constructive feedback provided by the three referees. We have carefully considered their comments and revised the manuscript to address the concerns raised, as detailed in our responses below. The most substantial revisions include updating the multiple linear regression (MLR) methodology to use standardized predictors and fitted intercepts, incorporating SHAP analysis to further evaluate predictor contributions, and clarifying the interpretation of the regression results. We have also expanded the discussion of aerosol size distributions and cloud-related aqueous-phase reactions, refined the interpretation of seasonal differences in organic aerosol formation and oxidation, and improved the organization and clarity of the manuscript. Additional figures, analyses, and supporting explanations have been included where appropriate. While these revisions have refined the quantitative results and their interpretation, the primary conclusions regarding the roles of photochemical oxidation and aqueous-phase reactions in coastal secondary organic aerosol formation remain supported. We believe these changes have strengthened the manuscript and improved the presentation of its findings. All revisions are documented in the Tracked Changes version of the manuscript submitted alongside this response.

Referee #1
GENERAL COMMENTS

This study aims to quantify the contribution that different mechanisms have on the formation of secondary organic aerosol (SOA), i.e., formation of SOA in the gas phase, in aqueous aerosol, and in cloud droplets. To address this question, the authors analyze data collected during the year-long EPCAPE field campaign in Southern California, USA. EPCAPE collected measurements of aerosol chemical composition and size distribution, gas chemical composition, meteorological and cloud-related parameters, and back-trajectory of air parcels. These measurements are subsequently analyzed using positive matrix factorization (PMF) to determine source apportionment, and multilinear regression (MLR) is used to determine the correlations and contributions of different variables to SOA formation. Sub-setting the data by season and air mass back-trajectory allows for identifying the patterns in season and regional influence, respectively.

The referee considers that the methodology used in this study to collect and analyze the data is rigorous. Furthermore, the referee considers that this study addresses an important and relevant question in the atmospheric sciences, and publishing this study in Atmospheric Chemistry and Physics would contribute to the atmospheric science research community.

The referee's primary critique of this study concerns the multivariate linear regression, which is described in the Specific Comments section.

SPECIFIC COMMENTS

Critiques on multivariate linear regression:

1. Why are the predictor variables normalized? What is physical and mathematical reasoning behind it?

   We thank the referee for this comment. We have revised the MLR analysis to use z-score standardization rather than min-max normalization. Section 2 (Methods), Section 4 (Multiple Linear Regression Analyses), Section 5 (Conclusions), and the abstract have been revised to reflect these changes. The predictor variables have different units and ranges, and standardization places them on a common scale so that their regression coefficients can be directly compared. This is particularly important for calculating the relative predictor contributions from the regression coefficients. We have clarified this rationale in the revised Section 2.6 in the Methods:

   New Lines 223–235. "Multiple Linear Regression (MLR) was used to identify the dependence of organic oxidation and SOA mass concentrations on numerous variables for primary and secondary processes (X_p). Each observation *i* of the predictor variables ($X_{i,p}$) was standardized using z-score standardization prior to regression:

$$Z_{i,p} = \frac{X_{i,p} - \mu_p}{\sigma_p} \quad (1)$$

   where μ_p is the mean of the predictor X_p and σ_p is the standard deviation of predictor X_p. MLR models were then fit using the fitlm() function from MATLAB:

$$Y = b + m_1 Z_1 + m_2 Z_2 + \cdots + m_p Z_p \quad (2)$$

   where *b* is the intercept, m_p are the regression coefficients corresponding to the standardized predictor variables Z_p, and *Y* represents the model-predicted value. Standardization allows regression coefficients for predictors with different units and ranges to be directly compared, with the slope m_p representing the change in the predicted variable for a one-standard-deviation increase in X_p. The relative contribution from each component is then represented as its regression coefficient m_p divided by the sum of the magnitudes of the regression coefficient terms."

2. If the predictor variables (X1, X2, etc.) are normalized, shouldn't the predicted variable (Y) also be normalized?

   Standardization of the predictor variables does not require standardization of the predicted variable. The predictors were standardized specifically to allow comparison of their regression coefficients. The predicted variable was retained in its original units so that the predicted OA factor mass concentrations and O/C, as well as the corresponding model errors (e.g., root mean square errors), remain directly interpretable. Standardizing the predicted variable would rescale the regression coefficients and predictions but would not be necessary for comparing the relative contributions of the standardized predictors.

3. In order to stay consistent with Equation 1, and to further emphasize that the multivariate linear regression is being fed normalized predictor values, shouldn't the predictor variable in Equation 2 have the subscript "norm", i.e., be "Xi,norm" instead of just "Xi"? Also, for consistent notation, in Line 1088, the average should read "Xi,norm", not "Xnorm,i".

We thank the referee for this comment. With the revised analysis, we have now defined the standardized value of each observation *i* of predictor X_p as $Z_{i,p}$ in Equation 1 with Z_p now appearing in equation 2 for consistency. The previous notation for the normalized predictor values has been removed from the revised manuscript.

4. Line 208 and 209. As a consequence of the previous comment, the subscripts in the text should include "norm", i.e. they should read "… normalized predictor value (Xp,norm)…" and "… all mpXp,norm predictor terms …".

   We agree and have updated the corresponding text to use the revised standardized predictor notation. The previous normalized terms have also been removed following revision of the contribution calculation.

5. The referee understand that the researchers have the freedom to make assumptions in how to best model a multivariate regression. However, could you please provide some reasoning as to why the intercept (b) in the regression is set to zero? And if it is not set to zero, does it change the final conclusions of this study?

   We thank the referee for raising this point. As part of the revised analysis using standardized predictors, we repeated the MLR with and without a fitted intercept. Following standardization, each predictor has a mean of zero. Therefore, when all standardized predictors are equal to zero, the predicted value is equal to the fitted intercept. Since the predictors are centered at zero, this intercept corresponds to the mean of the predicted variable. In contrast, fixing the intercept at zero forces the model to predict a value of zero when all predictors are at their mean values. This produces an offset between the measured and predicted values and substantially increases the root mean square error (RMSE). Fitting the intercept does not change the regression coefficients or the relative contributions calculated from these coefficients. We therefore revised the MLR to include a fitted intercept, and the fitted intercepts are now reported in Table 1 in the manuscript. The conclusions have also been updated based on the results of the revised standardized MLR analysis.

6. Line 498. The correlations in Figure 7f are described as "strong" with R values of 0.43 and 0.49. However, Line 111 defines a strong correlation as one with $R \geq 0.8$. Please ensure that the terminology used to describe correlation strength is consistent throughout the manuscript.

   We thank the referee for pointing this out. The original text has been replaced in the revised manuscript, and we have ensured that the terminology used to describe correlation strength is consistent throughout the manuscript.

Other critiques:

1. Line 18. Perhaps it is better to use the phrase “cloud processes” instead of “in-cloud reactions” because the bimodal nature of the size distribution is not due to chemical reactions alone; it is also due to the process of scavenging, which is a physical, not chemical, process (Dedrick et al., 2026).

   We thank the referee for raising this point. We agree that the bimodal size distribution may reflect both aqueous-phase reactions and physical scavenging of Aitken-mode particles (Dedrick et al., 2026). We have therefore revised the Abstract to use the broader term “cloud-related processes.” In the manuscript, we use “cloud processes” when referring to the bimodal size distribution and Hoppel minimum, while retaining “aqueous-phase reactions” when discussing higher SR-OOA and MO-OOA concentrations because scavenging alone cannot explain an increase in OOA mass concentrations. We have maintained this distinction throughout the revised manuscript.

2. Line 50. The phrase “photochemical oxidation” is used at the beginning of the sentence and then “photochemical aging” is used at the end. Are the authors using these two phrases interchangeably? If so, please consider using consistent terminology.

   We agree that while photochemical oxidation and aging are often used interchangeably, we should use consistent terminology. We changed “photochemical aging” to “photochemical oxidation” in New Line 56.

3. Line 162. Line 110 says that CVI measurements were excluded from this study. Please clarify.

   We thank the referee for pointing out this ambiguity. CVI measurements were excluded from the analyses presented in this study but were included with the ambient measurements in the dataset used for PMF. We have clarified this distinction in the revised manuscript:

   New Lines 174–176. “Out-of-cloud and CVI measurements were included in the combined dataset used for PMF to resolve factors consistently across both sampling conditions; this study focuses on out-of-cloud conditions.”

   Figure 2. The three-month periods used to calculate the seasonal averages differ slightly from the traditional definitions of meteorological seasons (NOAA). The referee recognizes that this difference is unlikely to affect the study’s findings; however, please explain the rationale for using these alternative three-month periods.

   We thank the referee for noting this distinction. The seasonal periods used here follow two previous EPCAPE studies (Han et al., 2025; Dedrick et al., 2026) and were selected to reflect the characteristic seasonal meteorology of coastal San Diego. In particular, low coastal stratiform clouds are prevalent during late spring and early summer, while warmer conditions typically occur later in summer and extend into early fall (Clemesha et al., 2016).

We have clarified the seasonal definitions and their rationale in the revised manuscript in the first paragraph of the Results section:

New Lines 244–246. “Seasons were defined as winter (January–March), spring (April–June), summer (July–September), and fall (October–December) to reflect the characteristic seasonal meteorology of coastal southern California (Han et al., 2025; Dedrick et al., 2026)”

4. Figure 7a–e. Because the correlation coefficient is used in the text to characterize the relationships shown in these subplots, the referee suggests including the corresponding R (or R^2) values in Figures 7a–e for clarity.

   We thank the referee for this suggestion. We have added the corresponding R^2 values found in Table 1 to Figures 7a–e (now Figure 8a–e) for clarity.

5. Figure 7 caption. Since measured O/C is on the x-axis, the correct description for Figure 7f should be “O3 vs O/C”, rather than “O/C vs O3”. The same correction applies to Figure 7g–j. We thank the referee for catching this. The Figure 7 (now Figure 8) caption has been updated accordingly.

6. Figure 7a and 7f. The time scales used in subplot (f) are annual, fall, and spring time scales. However, the time scales for the other subplots (g)–(j) are not specified. For clarity, could you please specify the time scale used in each subplot?

   The time periods for panels (g)–(j) were not previously specified because they correspond to the same seasons used for the respective MLR models in panels (b)–(e). We have now explicitly stated that the time scales in panels (g)–(j) are the same as those in (b)–(e) in the Figure 7 (now Figure 8) caption for clarity.

7. Figure 8. Could the authors please clarify the purpose of the red polynomial fits shown in subplots (k)–(t) and explain why they are not discussed in the text? The referee suggests either removing these fits if they are not essential to the analysis or providing a brief explanation of their purpose and interpretation in the text.

   We thank the referee for this suggestion. The red polynomial fits are included to highlight the size-dependent trends in f_{44} and the organic fraction of NR aerosol mass and facilitate comparison with relationships used to identify organic aerosol oxidation and condensation mechanisms (Liu et al., 2011; Maria et al., 2004). We have added this explanation to the text and clarified the purpose of the polynomial fits in the Figure 8 (now Figure 10) caption:

   New Lines 598–600 (Section 4.1). “Polynomial fits are included to highlight these size-dependent trends and facilitate comparison with relationships used to identify organic aerosol oxidation and condensation mechanisms (Liu et al., 2011; Maria et al., 2004).”

The description of the polynomial fit in the Figure 8 (now Figure 10) caption is revised to: "Red lines represent polynomial fits to the measured size-dependent relationships for comparison with the oxidation and condensation mechanisms described by Maria et al. (2004) and Liu et al. (2011)."

TECHNICAL COMMENTS

1. Line 111. Are the definitions of "weak", "moderate", and "strong" in terms of R or the absolute value of R (|R|)? In Line 578, the absolute value notation is used.

   We thank the referee for pointing this out. The definitions are in terms of the absolute value of R. We have now updated the manuscript in New Lines 122–123 to use the correct notation.

2. Line 131. There should be a dash in "high-resolution".

   We have now updated "high resolution" to include a dash in New Line 142.

3. Line 132. The negative sign in "I-" must be superscripted.

   The negative sign in I- is now superscripted in new Line 143.

4. Lines 188, 506, 507. Please use the en dash for range of numbers, and the dash for negative numbers.

   We have updated Line 188 (New Line 210) to use an en dash. The text previously appearing in Lines 506–507 has been removed during revision of the manuscript.

5. The in-text citations must have a space after the semicolon.

   We thank the referee for noting this formatting issue. We have therefore manually corrected the in-text citations throughout the manuscript to include a space after each semicolon.

6. The bibliography should use a consistent formatting. For instance, currently some references capitalize the name of the journal while others don't.

   We thank the referee for catching this. We have revised the bibliography to ensure consistent formatting of journal names throughout.

Referee #2

Based on observations from the Eastern Pacific Cloud Aerosol Precipitation Experiment (EPCAPE), this study investigated the seasonal contributions of photochemical and aqueous-phase oxidation to biogenic and mixed combustion organic aerosol (OA) in coastal Southern California. These findings are valuable for elucidating the relative roles of these oxidative

processes in OA formation within coastal environments. Here I have some suggestions for authors to further clarify their results as the below:

1. Given that SR-OOA is primarily driven by marine biogenic sources and daytime sea-breezes transporting marine-influenced air masses inland, why does its diurnal cyclepeak in the evening? (Fig. 2a–e)?

   We thank the referee for raising this point. The evening maximum in SR-OOA is consistent with the previously reported diurnal wind pattern during EPCAPE. Previous analysis of EPCAPE meteorology showed that northwesterly sea-breeze conditions typically developed between 08:00 and 10:00 local time, while the transition to easterly land-breeze conditions generally occurred between 18:00 and 20:00 (Han et al., 2025). The SR-OOA peak at approximately 18:00 occurs near the end of the daytime sea-breeze period, following several hours of sustained transport of marine-influenced air to Mt. Soledad. The evening maximum likely reflects the cumulative influence of daytime marine transport and atmospheric processing rather than maximum production at 18:00. Sulfate, which is also associated with marine biogenic sources during EPCAPE, shows a similar evening maximum, further supporting this interpretation.

2. Why does the minimum of O3 appear in summer(August), rather than in winter? (Fig.3a). This is contradictory to the daily mean downwelling shortwave radiation (DSW) peaking during summer.

   Although DSW peaks during summer, ozone concentrations reflect the balance between photochemical production and destruction rather than solar radiation alone. At coastal sites such as Mt. Soledad, marine boundary layer influence can result in faster photochemical destruction of ozone during summer, producing a characteristic late-summer minimum, while northern midlatitude sites can also exhibit a secondary ozone maximum in late fall (Parrish et al., 2016). This seasonal behavior explains why ozone concentrations at Mt. Soledad are lowest during summer despite peak summer DSW. We have revised the manuscript to include this discussion:

   New Lines 415–422. “Peak daily mean downwelling shortwave radiation (DSW) occurred during summer (235 ± 324 W m^{-2}), despite lower ozone (31 ± 7.3 ppb) and LO-OOA (0.12 ± 0.28 μg m^{-3}) concentrations (Table S7). A reduction of photochemical efficiency by the increased local cloud fraction in May (0.69 ± 0.39, Fig. 3d) may partially contribute to these summer minima but does not fully explain the patterns given the concurrent maximum in DSW. At coastal sites such as Mt. Soledad, marine boundary layer influence can result in faster photochemical destruction of ozone during summer, producing a characteristic late summer minimum despite greater solar radiation (Parrish et al., 2016). The concurrent decrease in LO-OOA suggests that higher summertime photochemistry may contribute to LO-OOA loss through photochemical removal or transformation to a more oxidized OA component.”

New Lines 859–862. “In contrast, local cloudiness coincided with reduced ozone and LO-OOA concentrations, consistent with reduced photochemical oxidation as well as increased marine boundary layer influence represented by greater cloudiness, where enhanced photochemical destruction can contribute to lower ozone concentrations (Parrish et al., 2016).”

SI: “This distinction is particularly important at the coastal Mt. Soledad site, where ozone concentrations reflect both photochemical production and destruction. Marine boundary layer influence can result in faster photochemical destruction of ozone during summer, producing a characteristic late summer minimum despite greater solar radiation (Parrish et al., 2016).”

3. The organic and inorganic components had very low diurnal variability across seasons due to the daily land-sea breeze transitions characteristic of the coastal environment as well as frequent daytime cloudiness reducing the role of photochemically driven changes (Han et al., 2025) (L352-355). This sentence is very abrupt. I can’t follow the logic between it and the surrounding sentences.

   We revised this sentence to clarify the connection between the weak summer MO-OOA diurnal cycle and the similarly low diurnal variability of AMS NR organic and inorganic components. The revised text now reads:

   New Lines 403–406. “The weak diurnal cycle observed for MO-OOA during summer is similar to those of AMS NR organic and inorganic components, which was attributed to daily land-sea breeze transitions as well as frequent daytime cloudiness reducing the role of photochemically driven changes (Han et al., 2025).”

4. Peak daily mean downwelling shortwave radiation (DSW) occurred during summer (235 ± 324 W m-2, Table S7), but LO-OOA concentrations remained low, suggesting a reduction of photochemical efficiency by the increased local cloud fraction in May (0.69 ± 0.39, Fig. 3d) (L363-366). I can't agree with this explain. The photochemical efficiency is closely related to DSW.

   We agree that reduced photochemical efficiency associated with increased local cloudiness alone cannot explain why both ozone and LO-OOA concentrations are lowest during summer, because DSW reaches its seasonal maximum during summer. However, local cloudiness may contribute to some degree. This is supported by the SOU trajectories, which were associated with 21% higher LCF, 31% lower DSW, 21% lower ozone, and 17% lower LO-OOA than the campaign average. These relationships indicate that increased cloudiness and the associated reduction in solar radiation can contribute to lower photochemical production of LO-OOA and ozone. However, because summer DSW remains high, this mechanism cannot fully explain the seasonal minimum. As discussed in Response #2, marine boundary layer influence can also result in faster photochemical destruction of ozone

during summer despite greater solar radiation (Parrish et al., 2016). The concurrent summer minimum in LO-OOA suggests that enhanced summertime photochemistry may similarly contribute to LO-OOA loss through photochemical removal or transformation to a more oxidized OA component. As reported in Response #2, we have revised these lines as such:

New Lines 415–422. “Peak daily mean downwelling shortwave radiation (DSW) occurred during summer (235 ± 324 W m^{-2}), despite lower ozone (31 ± 7.3 ppb) and LO-OOA (0.12 ± 0.28 μg m^{-3}) concentrations (Table S7). A reduction of photochemical efficiency by the increased local cloud fraction in May (0.69 ± 0.39, Fig. 3d) may partially contribute to these summer minima but does not fully explain the patterns given the concurrent maximum in DSW. At coastal sites such as Mt. Soledad, marine boundary layer influence can result in faster photochemical destruction of ozone during summer, producing a characteristic late summer minimum despite greater solar radiation (Parrish et al., 2016). The concurrent decrease in LO-OOA suggests that higher summertime photochemistry may contribute to LO-OOA loss through photochemical removal or transformation to a more oxidized OA component.”

5. The current organization of Section 3.2could be improvedto enhance logical flow.
We thank the referee for this suggestion. We have revised Section 3.2 to make the logical progression of the discussion more explicit. The introductory paragraph now states that the discussion progresses from factors associated with cloud aqueous reactions (SR-OOA and MO-OOA) to those more strongly associated with photochemical oxidation (LO-OOA) and combustion-related sources (C-OOA and HOA):

New Lines 352–355. “The following discussion evaluates the seasonal and diurnal variability of the OA factors together with these tracers, progressing from the factors associated with cloud aqueous reactions (SR-OOA and MO-OOA) to those more strongly associated with photochemical oxidation (LO-OOA) and combustion-related sources (C-OOA and HOA).”

The SR-OOA paragraph evaluates its seasonal and diurnal variability, correlations with UCVF, and association with bimodal size distributions as evidence of cloud processes including aqueous-phase reactions. The following two paragraphs discuss the seasonal and diurnal behavior of MO-OOA and evidence for contributions from both cloud aqueous and regional photochemical processes. The LO-OOA paragraph then evaluates its seasonal and diurnal behavior and relationships with ozone and DSW, supporting a stronger association with local photochemical production. Finally, the C-OOA and HOA paragraphs examine their seasonal variability and relationships with rBC before distinguishing the more oxidized C-OOA from HOA associated with local traffic emissions. We also combined two short paragraphs describing the September maximum and fall behavior of C-OOA and HOA and the concurrent increase in rBC to provide a more continuous discussion of their seasonal variability and combustion-related influences.

6. Section 3.3, a figure showing the back-trajectories is recommended, which helps to distinguish different air masses.

We thank the referee for this suggestion. We have added a figure showing the cluster centroid back-trajectories for each of the five air-mass groups to the Supplement (Figure S10), which helps distinguish the different air-mass groups discussed in Section 3.3.

7. It is hard to understand that "Ozone has a stronger contribution to variability during winter (58%) and fall (70%), and a smaller role during spring (15%) and summer (30%)" (L504-505). Same as Q2.

   The MLR analysis has been replaced with the revised analysis using z-score standardized predictors, so the quoted results are no longer included in the manuscript. In the updated analysis, the percentages represent the relative MLR contributions of the predictors to the modeled O/C, which is based on regression coefficients, rather than contributions to variability, since variability is based on squared Pearson correlation coefficients (R^2). Each predictor is standardized such that a one-unit change represents a one-standard-deviation increase in that predictor. The resulting regression coefficient represents the change in modeled O/C associated with a one-standard-deviation increase in the predictor while holding the other predictors constant. The relative MLR contributions are calculated from these standardized regression coefficients relative to the sum of their absolute values. Ozone now provides the largest contribution to organic oxidation (O/C) during winter (56%), summer (50%), and fall (37%), while UCVF provides the largest contribution during spring (61%).

8. The conclusionsshould be refinedto better highlight the key findings.

   We thank the referee for this suggestion. We have revised and reorganized the Conclusions to more clearly highlight the key findings and reduce repetition among the different analyses. The first paragraph briefly summarizes the scope of the study and the five OA factors identified. We then combine the seasonal, diurnal, and air mass origin results into a single paragraph that highlights the primary formation pathways identified for each factor. The following paragraph summarizes the MLR results for O/C and the relative roles of photochemical and aqueous oxidation, followed by a paragraph integrating the MLR and simple regression results for the individual PMF factors and quantifying their distinct and seasonally varying formation pathways. We then place these findings in the context of previous studies, highlighting the distinction between aerosol water, local cloud, and upwind in-cloud aqueous oxidation considered in this study, while also clarifying the limitations of using these tracers to represent broader oxidation processes. Finally, the last paragraph of the Conclusions describes the overall significance of the results for understanding the effects of source type, season, and transport history on coastal SOA formation and oxidation and their relevance to aerosol hygroscopicity and cloud condensation nuclei activity.

Referee #3

This manuscript presents a useful year-long dataset on organic aerosol composition at a coastal site in Southern California. The combined analysis of PMF factors, chemical tracers, and upwind cloud conditions is interesting and relevant to ACP. However, I have concerns about how the size distributions and regression results are interpreted. I recommend major revision.

Major comments

1. The size distributions in Fig. 1 need clearer explanation. From the caption, these are total particle number distributions during periods when one PMF factor exceeds its 80th percentile, rather than size distributions of the individual factors. Please make this distinction explicit in the Methods and discussion. The authors should report the number of observations in each group and check whether the differences persist within comparable seasons and air masses. A Hoppel gap suggests cloud processing, but does not necessarily show that the associated organic factor was formed in cloud water.

   As already described in the Methods, the particle number size distributions (PNSDs) in Figure 1 are ambient aerosol size distributions measured by the SEMS and APS. The original discussion also explicitly identifies the bimodal number size distributions as originating from the merged SEMS and APS measurements:

   Old Lines 316–319. “Bimodal number size distributions from merged SEMS and APS measurements, which are more frequent during summer (Dedrick et al., 2026), are associated with elevated SR-OOA concentrations (Fig. 1b), suggesting that the aqueous-phase reactions that contributed to SR-OOA formation also contributed to particle growth in forming the “Hoppel gap” as a result of cloud processing (Hoppel et al., 1990).”

   The original Figure 1 caption further specifies that the median PNSDs are shown during periods when each PMF factor mass concentration exceeded its 80th percentile and was unique to that factor, defined as periods when the other PMF factors were not simultaneously above their respective 80th percentiles. Figure 1 shows ambient PNSDs associated with elevated concentrations of each PMF factor rather than size distributions of the individual PMF factors. Particle number size distributions of the AMS PMF factors cannot be obtained from these measurements because the PMF factors are resolved from AMS organic mass spectra, whereas particle number size distributions are measured independently by the SEMS and APS. Consequently, the PNSDs in Figure 1 could not solely be the measured number size distributions of individual AMS PMF factors. To eliminate any remaining ambiguity, we have revised the discussion to state explicitly that the SEMS/APS measurements are of ambient aerosol during periods when the corresponding PMF factor uniquely exceeded its 80th percentile:

   New Lines 365–367. “Bimodal number size distributions, which are more frequent during summer (Dedrick et al., 2026), were observed from merged SEMS and APS measurements during periods when SR-OOA concentrations uniquely exceeded their 80th percentile (Fig. 1b).”

In response to the referee's request, we have also added the number of PNSD observations (N) contributing to each distribution directly to Figure 1 and clarified this in the figure caption. We additionally evaluated the PNSDs separately by season and trajectory to determine whether the observed associations persisted under comparable conditions. Bimodal distributions were consistently observed for well-sampled groups (>100 PNSD observations). In particular, SR-OOA was associated with bimodal PNSDs during spring and summer. SR-OOA concentrations were lower during winter and fall, resulting in substantially fewer periods when SR-OOA uniquely exceeded its 80th percentile (N = 60 and 57, respectively) (Fig. R1). The winter distribution remained generally bimodal but was substantially noisier, while the fall distribution was unimodal. MO-OOA similarly showed consistent associations with bimodal PNSDs across all seasons.

Separating by trajectory showed the same general behavior (Fig. R2). SR-OOA was associated with bimodal PNSDs for the CNW, LALB, and SOU trajectories. No unique high-SR-OOA observations occurred for the EAS or MWE trajectories, precluding evaluation of those trajectory groups. MO-OOA was also associated with bimodal PNSDs for the CNW, LALB, and SOU trajectories. The EAS and MWE subsets contained only 34 and 1 observations, respectively, and therefore had too few observations for meaningful comparison. Thus, the association of elevated SR-OOA and MO-OOA with bimodal PNSDs persisted when the data were stratified by both season and trajectory where adequate observations were available, despite bimodal distributions being more frequent during summer, indicating that the association was not solely driven by seasonal differences in PNSD.

We agree with the referee that the presence of a Hoppel minimum alone does not demonstrate that the associated organic factor was formed in cloud water. We have therefore revised the discussion to clarify that the bimodal size distributions provide supporting evidence of cloud-related processes, which may include both aqueous-phase reactions and physical scavenging, rather than independently demonstrating aqueous-phase formation. We retain the interpretation of aqueous-phase formation and oxidation when discussing the higher SR-OOA and MO-OOA concentrations associated with cloud-related conditions, as physical scavenging alone would not explain an increase in OOA mass. We also expanded the discussion of previous marine observations to clarify how associations between bimodal size distributions, oxidized OA, and aqueous-phase oxidation support this interpretation:

New Lines 367–376. "The Hoppel minimum in these distributions provides additional evidence of cloud processes (Hoppel et al., 1990), further supporting the association of SR-OOA with in-cloud aqueous-phase reactions inferred from its relationships with UCVF. While the bimodal distributions alone do not demonstrate that SR-OOA was formed in cloud water, the association of bimodal distributions and SR-OOA, which had the second-highest O/C of the resolved OA factors (O/C = 1.00), is consistent with observations of oxidized OA and aqueous-phase reactions in other marine environments. Heutte et al. (2025) similarly

reported that Arctic OOA was associated with bimodal size distributions containing a Hoppel minimum that could result from aqueous-phase reactions. At Ascension Island and over the southeast Atlantic, bimodal size distributions indicative of cloud processes were also observed together with highly oxidized OA, with aqueous-phase reactions suggested to contribute to OA oxidation (Dobracki et al., 2025; Che et al., 2022)."

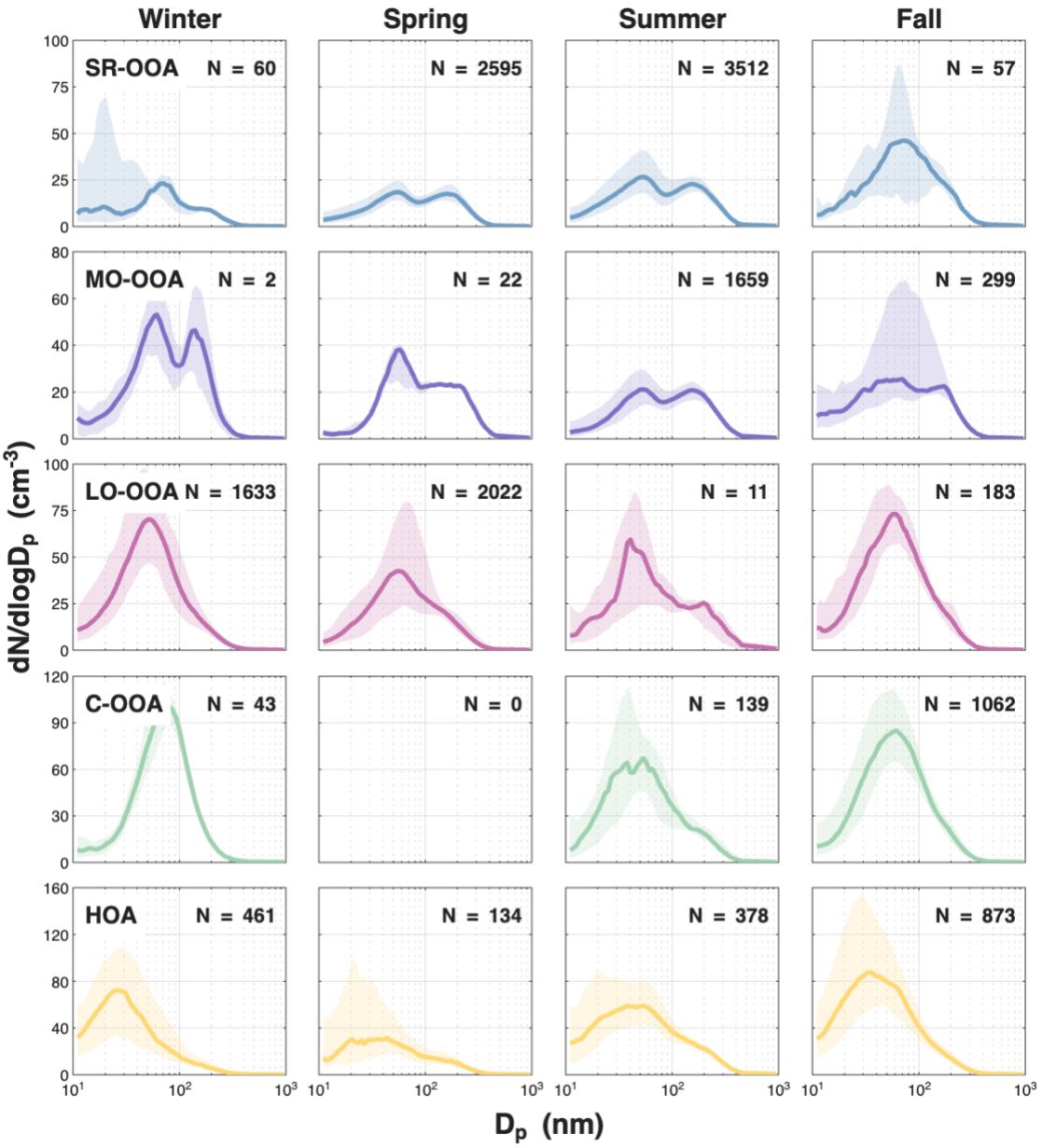


Figure R1. The median particle number size distributions from the merged SEMS and APS measurements during periods when PMF factor mass concentrations exceeded their 80th percentile and were unique to that factor (i.e., not simultaneously above the 80th percentile for the other PMF factors) are shown for each season. Shaded regions represent the IQR. The number of PNSD observations contributing to each distribution is indicated by N. Mass concentrations exclude times with particle number concentrations exceeding 8000 cm^{-3}.

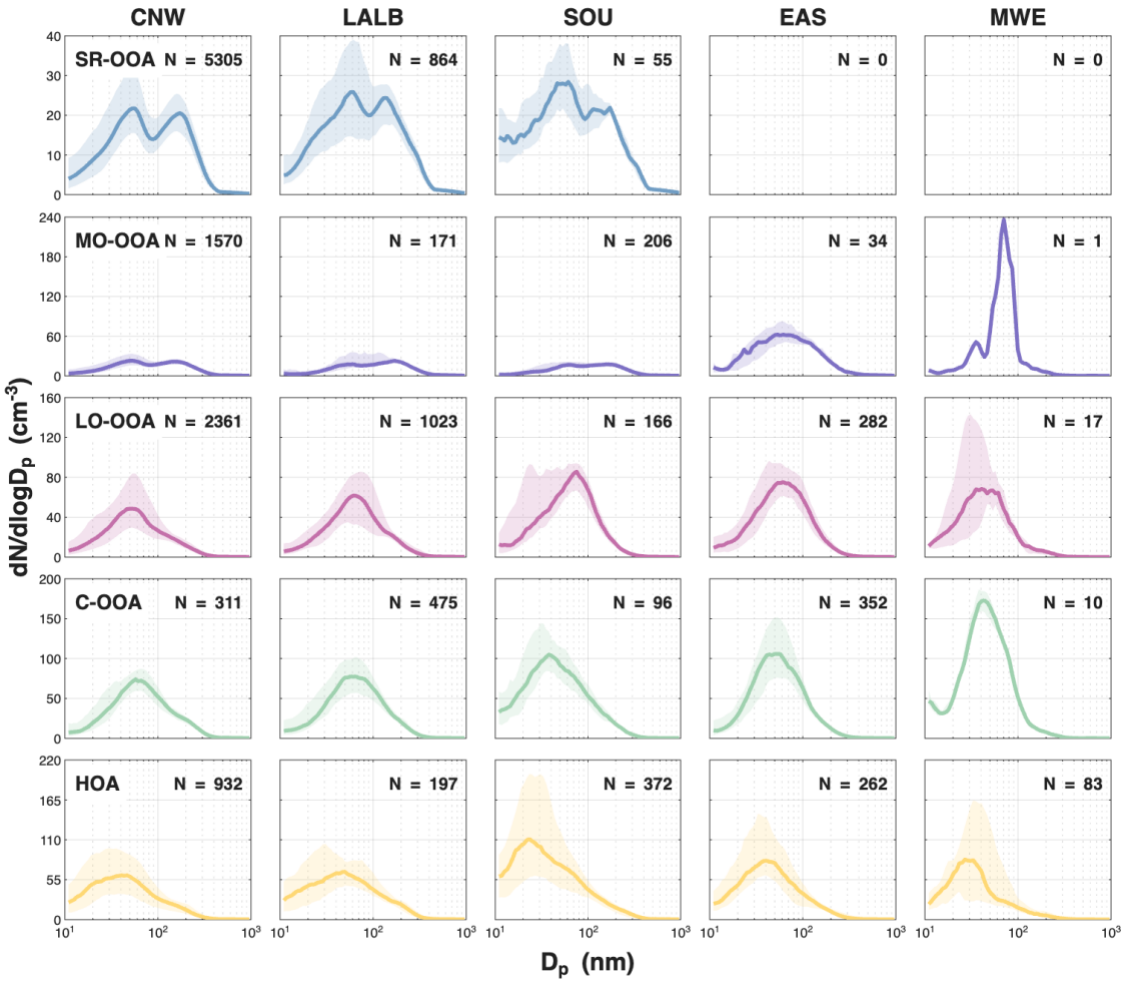


Figure R2. The median particle number size distributions from the merged SEMS and APS measurements during periods when PMF factor mass concentrations exceeded their 80th percentile and were unique to that factor (i.e., not simultaneously above the 80th percentile for the other PMF factors) are shown for each back-trajectory. Shaded regions represent the IQR. The number of PNSD observations contributing to each distribution is indicated by N. Mass concentrations exclude times with particle number concentrations exceeding 8000 cm^{-3}.

2. My main concern is the interpretation of the MLR percentages as contributions from different formation pathways. The calculation based on regression coefficients multiplied by mean normalized predictors is not a partitioning of explained variance or SOA production. Thus, statements such as “70% of SR-OOA formation” being attributed to upwind cloud reactions appear too strong. Please clarify what these percentages represent and revise the Abstract, Conclusions, and corresponding figures accordingly.

   We appreciate the referee’s concern and agree that the MLR-derived percentages are not a partitioning of explained variance. However, the percentages were intended to represent the relative contributions of the selected formation pathways to the modeled organic aerosol factor concentrations, consistent with the MLR approach previously applied to EPCAPE aerosol measurements by Maneenoi et al. (2025). In that study, variables were standardized to a common scale and the fitted regression coefficients were used to derive the relative

contributions associated with each source or process indicator. The resulting coefficients were then interpreted as relative contributions of photochemical, cloud water and aerosol water aqueous oxidation to sulfate production. A similar MLR-based approach has been applied by Dong et al. (2024), who used O_3 and RH as indicators of gas-phase photochemical and aqueous-phase oxidation and quantified their relative contributions to saturated dicarboxylic acid formation from the corresponding regression coefficients. Importantly, the pathway contributions from these studies were reported separately from the variability explained by the MLR. The percentages reported here represent the relative contributions of the selected formation pathways to the modeled OA factor concentrations and are distinct from the fraction of variability explained by the MLR, which is given by R^2. We identified instances in the manuscript where these MLR contributions were incorrectly described as explaining a percentage of OA factor variability. We have revised these statements throughout the manuscript to refer to the MLR contributions to PMF factor production or organic oxidation (O/C) rather than variability and have clarified that model performance, reported as R^2, separately represents the squared Pearson correlation between the measured and predicted values.

In response to the referee's concern, we have also added Shapley Additive Explanations (SHAP) analysis (in Response #3) as an additional, independent metric for evaluating the relative contributions of the predictor variables to the modeled OA factor concentrations. SHAP is a model-interpretation method based on Shapley values that quantifies the contribution of each predictor to individual model predictions relative to a reference prediction. The SHAP-derived contributions therefore provide a complementary measure of predictor importance that can be compared with the relative contributions derived from the MLR coefficients. Following z-score standardization, the MLR-based and SHAP-derived contributions differed by only 2% on average, compared with an average difference of 14% when min–max normalization was used. This closer agreement indicates greater consistency between the MLR-based contributions and the independent SHAP assessment following z-score standardization (Response #3).

3. The regression setup also needs justification. Min–max normalization does not resolve non-normality, and linear regression does not require normally distributed predictors. Why was the intercept fixed at zero? After normalization, zero represents the observed minimum rather than the absence of the relevant process. Please compare the results with a model that includes an intercept. Table 1 reports uncentered R2 which should not be interpreted as the fraction of variability explained. Conventional R2 and an independent validation would provide a more informative assessment.

   We appreciate the referee's comments regarding the regression setup. We have revised the MLR analysis to address these concerns. First, the predictor variables are now standardized using z-scores rather than min-max normalization. Standardization places predictors with different units and ranges on a common scale, allowing the fitted coefficients to be compared directly, with each coefficient representing the change in the predicted variable associated with a one-standard-deviation change in the corresponding predictor.

We also repeated the analysis both with and without a fitted intercept. Because standardization centers each predictor at zero, inclusion of the intercept did not change the fitted slopes, MLR predictor contributions, or correlations between measured and predicted values. However, including the intercept substantially reduced RMSE because zero standardized predictor values represent mean predictor conditions rather than zero concentrations of the predicted aerosol component. For example, for the annual O/C model, RMSE decreased from 0.94 without an intercept to 0.14 with an intercept, while R^2 remained 0.33. Similar reductions in RMSE were observed for the OA factors. We therefore use the standardized model with a fitted intercept in the revised analysis.

We additionally revised the reported R^2 metric. Rather than the previously reported uncentered R^2, R^2 is now calculated as the square of the Pearson correlation coefficient (R) between the measured and MLR-predicted values. Thus, the reported R^2 quantifies the fraction of variability in the measured values associated with variability in the model predictions, while RMSE separately quantifies the magnitude of the prediction errors.

Table R1: Multiple linear regression (MLR) results showing standardized regression coefficients for predicted PMF factor mass concentrations (SR-OOA, MO-OOA, LO-OOA, C-OOA) and bulk O/C at Mt. Soledad. Predictor variables include ozone (O_3), upwind cloud vertical fraction (UCVF), relative humidity (RH), refractory black carbon (rBC), and local cloud fraction (LCF). Results are shown for models with and without a fitted intercept for annual, seasonal, and CNW trajectory subsets. Model performance is evaluated using squared Pearson correlations (R^2) and root mean square error (RMSE).

Predicted Variable	Intercept	Ozone	UCVF	RH	rBC	LCF	R^2	RMSE
O/C								
Annual	0.00	0.01	0.10	0.01	-0.01	-0.01	0.33	0.94
	0.92	0.01	0.10	0.01	-0.01	-0.01	0.33	0.14
Winter	0.00	0.05	0.01	0.00	0.02	0.01	0.16	0.78
	0.77	0.05	0.01	0.00	0.02	0.01	0.16	0.12
Spring	0.00	0.00	0.09	0.02	-0.03	-0.01	0.38	0.96
	0.95	0.00	0.09	0.02	-0.03	-0.01	0.38	0.13
Summer	0.00	0.06	0.01	0.01	-0.03	-0.01	0.27	1.05
	1.04	0.06	0.01	0.01	-0.03	-0.01	0.27	0.11
Fall	0.00	0.05	0.04	0.00	-0.03	0.01	0.42	0.84
	0.84	0.05	0.04	0.00	-0.03	0.01	0.42	0.10
Annual-CNW	0.00	0.02	0.09	0.02	-0.01	-0.01	0.26	0.98
	0.97	0.02	0.09	0.02	-0.01	-0.01	0.26	0.16
SR-OOA								
Annual	0.00	0.00	0.10	0.01	0.00	-0.01	0.28	0.27
	0.21	0.00	0.10	0.01	0.00	-0.01	0.28	0.17
Winter	0.00	0.03	0.01	0.01	-0.01	0.01	0.19	0.11
	0.08	0.03	0.01	0.01	-0.01	0.01	0.19	0.07
Spring	0.00	0.03	0.06	0.04	-0.01	-0.04	0.24	0.24
	0.21	0.03	0.06	0.04	-0.01	-0.04	0.24	0.13
Summer	0.00	0.01	0.09	-0.03	-0.03	-0.01	0.19	0.42
	0.36	0.01	0.09	-0.03	-0.03	-0.01	0.19	0.22
Fall	0.00	0.02	0.04	0.02	0.00	0.02	0.28	0.12
	0.07	0.02	0.04	0.02	0.00	0.02	0.28	0.10
Annual-CNW	0.00	0.00	0.11	-0.01	0.00	-0.01	0.22	0.31
	0.25	0.00	0.11	-0.01	0.00	-0.01	0.22	0.19
MO-OOA								
	0.00	0.20	0.13	0.25	0.32	-0.11	0.07	1.56

Annual	0.77	0.20	0.13	0.25	0.32	-0.11	0.07	1.36
Winter	0.00	0.05	0.03	-0.03	0.09	-0.04	0.39	0.25
	0.18	0.05	0.03	-0.03	0.09	-0.04	0.39	0.17
Spring	0.00	0.11	0.13	0.02	0.03	-0.02	0.36	0.35
	0.29	0.11	0.13	0.02	0.03	-0.02	0.36	0.20
Summer	0.00	1.36	-0.72	0.46	0.32	-0.02	0.38	2.49
	1.81	1.36	-0.72	0.46	0.32	-0.02	0.38	1.72
Fall	0.00	0.29	0.03	0.13	0.11	0.06	0.38	0.65
	0.53	0.29	0.03	0.13	0.11	0.06	0.38	0.38
Annual-CNW	0.00	0.23	0.07	0.29	0.34	-0.16	0.06	1.94
	0.98	0.23	0.07	0.29	0.34	-0.16	0.06	1.67
LO-OOA								
Annual	0.00	0.17	-0.06	0.02	0.04	-0.02	0.18	0.45
	0.24	0.17	-0.06	0.02	0.04	-0.02	0.18	0.38
Winter	0.00	0.02	0.09	-0.11	0.01	-0.05	0.09	0.71
	0.43	0.02	0.09	-0.11	0.01	-0.05	0.09	0.57
Spring	0.00	0.28	-0.01	0.00	0.12	-0.05	0.44	0.44
	0.26	0.28	-0.01	0.00	0.12	-0.05	0.44	0.35
Summer	0.00	0.08	-0.05	0.03	0.06	0.00	0.21	0.23
	0.12	0.08	-0.05	0.03	0.06	0.00	0.21	0.19
Fall	0.00	0.11	-0.03	0.06	0.07	-0.04	0.25	0.30
	0.21	0.11	-0.03	0.06	0.07	-0.04	0.25	0.22
Annual-CNW	0.00	0.15	-0.07	0.05	0.04	-0.02	0.19	0.39
	0.20	0.15	-0.07	0.05	0.04	-0.02	0.19	0.33
C-OOA								
Annual	0.00	-0.02	-0.01	0.08	0.35	-0.10	0.21	0.87
	0.53	-0.02	-0.01	0.08	0.35	-0.10	0.21	0.70
Winter	0.00	0.01	0.01	0.00	0.16	-0.02	0.56	0.18
	0.09	0.01	0.01	0.00	0.16	-0.02	0.56	0.15
Spring	0.00	-0.05	0.02	-0.02	0.01	-0.02	0.13	0.17
	0.10	-0.05	0.02	-0.02	0.01	-0.02	0.13	0.14
Summer	0.00	0.49	-0.35	0.16	0.29	0.01	0.33	1.34
	1.05	0.49	-0.35	0.16	0.29	0.01	0.33	0.83
Fall	0.00	0.15	-0.10	0.12	0.36	-0.08	0.35	1.03
	0.88	0.15	-0.10	0.12	0.36	-0.08	0.35	0.52
Annual-CNW	0.00	0.02	-0.01	0.11	0.30	-0.08	0.13	1.00
	0.54	0.02	-0.01	0.11	0.30	-0.08	0.13	0.84

Finally, because standardization centers each predictor at zero, the previous calculation based on the regression coefficient multiplied by the mean normalized predictor is no longer applicable. MLR predictor contributions are now calculated from the absolute magnitudes of the standardized regression coefficients, relative to the five predictors, to sum to 100%, with the coefficient sign retained to indicate the direction of the association. We also calculated SHAP-derived contributions as a complementary assessment of predictor importance. For each predictor, the mean absolute SHAP value across all observations was calculated and normalized by the sum of the mean absolute SHAP values across the five predictors, such that the absolute SHAP-derived contributions sum to 100%. The direction of each SHAP-derived contribution was determined from the relationship between the predictor values and their corresponding SHAP values: a positive sign indicates that higher predictor values are associated with higher SHAP values and therefore increase the model prediction, whereas a negative sign indicates that higher predictor values are associated with lower SHAP values and therefore decrease the model prediction. The magnitude of the SHAP-derived percentage represents the predictor's relative importance to the model predictions, while the

sign represents the direction of its association with the predicted OA factor concentration or O/C.

Overall, the MLR and SHAP-derived contributions were similar (Table R2), with both approaches identifying the same major predictor. Annual SR-OOA showed a strong UCVF contribution using both the MLR standardized coefficients (79%) and SHAP (81%), while annual LO-OOA showed the largest contribution from ozone (55% for both approaches). The largest difference between the two contribution estimates was 14% for rBC in the annual CNW C-OOA model (59% from the standardized coefficients and 45% from SHAP). Across the models, the largest differences were generally observed for rBC, where SHAP-derived contributions were lower than MLR standardized-coefficient contributions, whereas most predictor contributions differed by only a few percentage points between the two approaches. These results indicate that the relative pathway contributions are generally robust to whether they are quantified from MLR standardized regression coefficients or from their contributions to individual model predictions using SHAP.

Table R2: Multiple linear regression (MLR) results showing relative predictor contributions for predicted PMF factor mass concentrations (SR-OOA, MO-OOA, LO-OOA, C-OOA) and bulk O/C at Mt. Soledad. Predictor variables include ozone (O_3), upwind cloud vertical fraction (UCVF), relative humidity (RH), refractory black carbon (rBC), and local cloud fraction (LCF). MLR contributions are calculated from the absolute magnitudes of the standardized regression coefficients relative to the five predictors, with the coefficient sign retained to indicate the direction of the association. SHAP-derived relative contributions are given in parentheses and are calculated from mean absolute SHAP values relative to the five predictors, with the sign indicating whether higher predictor values are associated with higher or lower SHAP values. Results are the same for models with and without a fitted intercept for annual, seasonal, and CNW trajectory subsets.

Predicted Variable	Ozone	UCVF	RH	rBC	LCF
O/C					
Annual	6% (6%)	**77% (79%)**	5% (4%)	-5% (-3%)	-7% (-8%)
Winter	**56% (58%)**	12% (13%)	-1% (-2%)	24% (19%)	7% (9%)
Spring	3% (3%)	**61% (67%)**	11% (10%)	-18% (-12%)	-7% (-8%)
Summer	**50% (52%)**	8% (9%)	8% (8%)	-29% (-26%)	-5% (-6%)
Fall	**37% (38%)**	30% (32%)	-0% (-0%)	-23% (-18%)	10% (12%)
Annual-CNW	12% (11%)	**60% (63%)**	15% (14%)	-5% (-3%)	-8% (-10%)
SR-OOA					
Annual	-2% (-1%)	**79% (81%)**	11% (10%)	0% (0%)	-8% (-8%)
Winter	**40% (39%)**	16% (17%)	11% (11%)	-17% (-13%)	16% (19%)
Spring	18% (16%)	**33% (36%)**	22% (21%)	-4% (-2%)	-23% (-25%)
Summer	4% (4%)	**55% (57%)**	-16% (-16%)	-19% (-16%)	-6% (-7%)
Fall	21% (20%)	**38% (37%)**	21% (22%)	1% (0%)	19% (20%)
Annual-CNW	-3% (-3%)	**79% (80%)**	-7% (-6%)	-3% (-2%)	-9% (-10%)
MO-OOA					
Annual	20% (21%)	13% (15%)	**25% (25%)**	32% (24%)	-11% (-14%)
Winter	23% (24%)	13% (14%)	-12% (-14%)	**37% (29%)**	-15% (-20%)
Spring	35% (33%)	**43% (47%)**	7% (6%)	9% (5%)	-7% (-8%)
Summer	**47% (48%)**	-25% (-26%)	16% (16%)	11% (10%)	-1% (-1%)
Fall	**47% (47%)**	4% (5%)	20% (23%)	18% (14%)	10% (12%)
Annual-CNW	21% (22%)	6% (8%)	**27% (29%)**	31% (22%)	-14% (-19%)
LO-OOA					
Annual	**55% (55%)**	-18% (-20%)	7% (7%)	14% (10%)	-7% (-8%)

Winter	7% (7%)	32% (31%)	-40% (-40%)	4% (3%)	-17% (-20%)
Spring	**60% (63%)**	-3% (-4%)	0% (0%)	26% (19%)	-11% (-14%)
Summer	**35% (36%)**	-25% (-26%)	15% (15%)	25% (22%)	-0% (-0%)
Fall	**37% (37%)**	-10% (-10%)	20% (22%)	21% (16%)	-12% (-14%)
Annual-CNW	**46% (45%)**	-20% (-23%)	16% (17%)	11% (7%)	-7% (-9%)
C-OOA					
Annual	-3% (-4%)	-1% (-2%)	14% (16%)	**63% (53%)**	-18% (-25%)
Winter	5% (6%)	5% (7%)	1% (2%)	**78% (71%)**	-10% (-15%)
Spring	-39% (-37%)	**19% (21%)**	-19% (-19%)	6% (4%)	-17% (-19%)
Summer	**38% (39%)**	-27% (-29%)	12% (12%)	23% (20%)	1% (1%)
Fall	19% (20%)	-12% (-13%)	15% (18%)	**45% (36%)**	-10% (-12%)
Annual-CNW	3% (3%)	-2% (-2%)	22% (27%)	**59% (45%)**	-15% (-22%)

Figure R3 compares the MLR predictor contributions from the previous min-max-normalized model with those from the revised standardized-coefficient and SHAP approaches. The standardized annual SR-OOA remained strongly associated with UCVF, with its MLR contribution changing from 70% in the min-max-normalized model to 79% using standardized coefficients (81% using SHAP), while the annual LO-OOA ozone MLR contribution changed from 64% to 55% (55%). For C-OOA, the previously reported uncentered R^2 values from the min-max-normalized model were lower for the annual, annual-CNW, and spring models than for the winter, summer, and fall models. Although the revised R^2 is calculated differently, as the squared Pearson correlation between measured and predicted values, it shows the same relative pattern, with lower R^2 for annual (0.21), annual-CNW (0.13), and spring (0.13) than for winter (0.56), summer (0.33), and fall (0.35). The association between C-OOA and rBC was also present in the min-max-normalized model: rBC had the second-largest MLR contribution in the annual and annual-CNW models and the largest MLR contribution during winter (49%). The primary change in the revised C-OOA MLR contributions is the reduced MLR contribution associated with RH, which was 53% in the annual model, 42% in the annual-CNW model, and 37% for the spring model in the min-max-normalized analysis. Thus, the larger MLR contribution of rBC in the revised annual and annual-CNW models reflects a redistribution of the predictor MLR contributions following standardization rather than a newly identified C-OOA-rBC relationship. Section 4.4 has been rewritten to better represent C-OOA contributions.

For MO-OOA, winter was the only season where standardization changed the predictor with the largest MLR contribution, from ozone (46%) in the min-max-normalized analysis to rBC (37%) using standardized coefficients. The rBC MLR contribution increased from 9% to 37%, while the ozone contribution decreased from 46% to 23% when standardizing predictors. The correlations of winter MO-OOA with rBC (R = 0.43) and ozone (R = 0.30) were identical using the raw, min-max-normalized, and standardized predictors. Thus, the change in their estimated MLR contributions reflects differences in predictor scaling and the contribution calculation rather than changes in their underlying relationships with MO-OOA. In the previous approach, each regression coefficient was multiplied by the mean min-max-normalized predictor value. This calculation therefore estimated the magnitude of each modeled predictor term at its mean concentration within the observed range, rather than comparing equivalent changes among predictors. This distinction was particularly important

for winter rBC because its concentrations were generally low but highly variable. Winter and spring had the lowest median rBC concentrations (14 ng m^{-3}), while the winter mean was substantially higher (48 ± 118 ng m^{-3}) because of high-rBC measurements. The resulting large winter rBC range produced a mean min-max-normalized value of only 0.075, compared with 0.678 for ozone, which reduced the estimated rBC MLR contribution relative to ozone. Using the median normalized predictor value further reduced the rBC MLR contribution, consistent with the low typical winter rBC concentration. In the revised analysis, each standardized coefficient instead represents the predicted change in MO-OOA for a one-standard-deviation increase in the predictor, allowing equivalent standardized changes in the predictors to be compared on a common scale. The revised MLR contributions are also more consistent with the relative strengths of the observed relationships, as winter MO-OOA was more strongly correlated with rBC (R = 0.43) than with ozone (R = 0.30), consistent with the larger standardized MLR contribution from rBC (37%) than ozone (23%). These results support the standardized-coefficient approach as a more appropriate comparison of the relative MLR contributions of the predictors to MO-OOA production.

The O/C results showed a substantial change from the previous min-max-normalized analysis, with revisions to Section 4.1 reflecting these changes to better represent the results. In the annual model, the previous MLR contributions were distributed primarily between RH (39%) and ozone (38%), with a smaller contribution from UCVF (19%). In the revised standardized analysis, UCVF had the largest annual O/C contribution at 77% using the standardized coefficients and 79% using SHAP, while contributions decreased to 6% (6%) for ozone and 5% (4%) for RH. Although the annual O/C relationship was strongly associated with UCVF, the seasonal models indicate that the relative importance of UCVF and ozone varied throughout the year. Ozone had the largest contribution during winter (56%) and summer (50%), while UCVF had the largest contribution during spring (61%). During fall, ozone (37%) and UCVF (30%) both had substantial contributions, while the annual-CNW model was primarily associated with UCVF (60%).

Figures 9 and 10 (now Figures 7 and 9, respectively) have been updated to show the revised standardized-coefficient contributions for the annual and seasonal MLR models, with O/C now included in the seasonal analysis. Figure 9 (now Figure 7) highlights the seasonal variability in the MLR predictor contributions, particularly for O/C. Figure 10 (now Figure 9) has also been updated to compare the revised seasonal MLR contributions with the corresponding monthly Pearson correlations, providing an independent assessment of whether the seasonal relationships identified by the MLR are also evident in the observed correlations. In addition, the addition of SHAP analysis provides a complementary evaluation of the relative predictor contributions, which generally identifies the same major predictor relationships as the standardized regression coefficients.

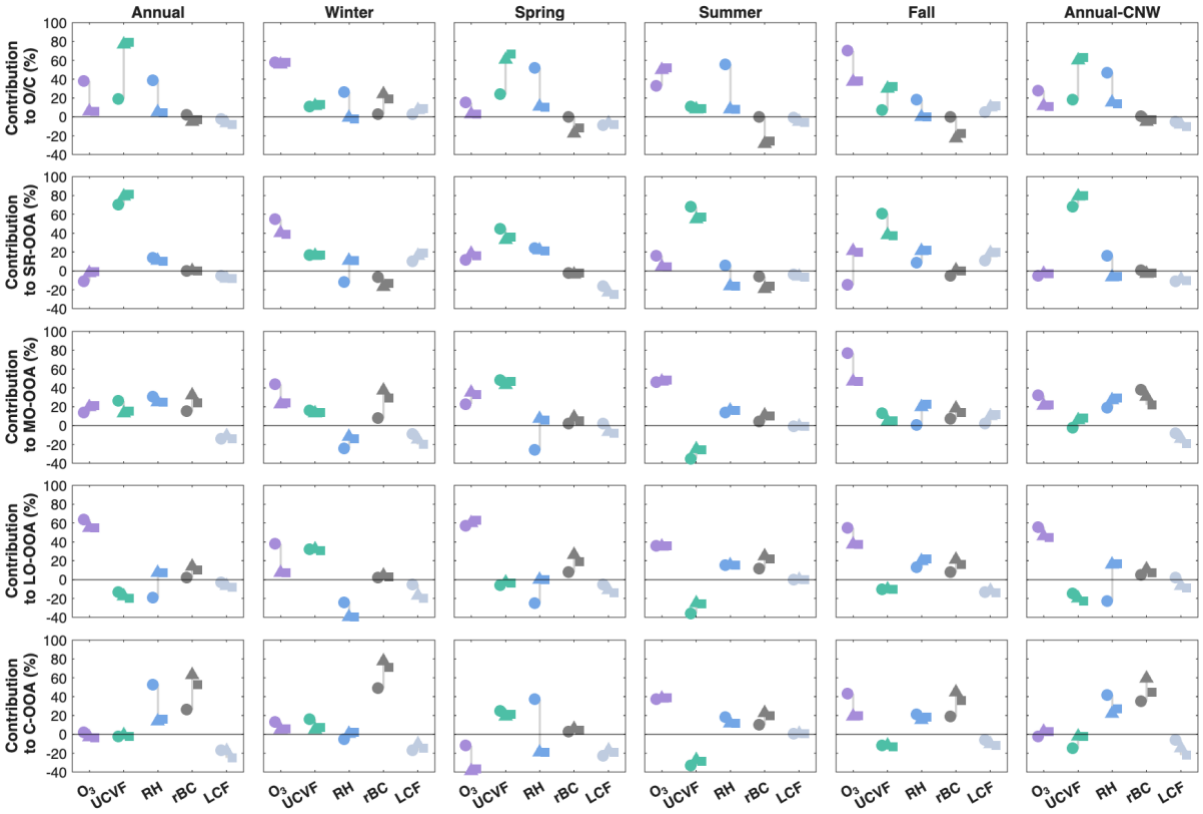


Figure R3. Comparison of relative predictor contributions to O/C, SR-OOA, MO-OOA, LO-OOA, and C-OOA for the annual, seasonal, and annual coastal northwesterly (CNW) models. Contributions are shown for O_3, upwind cloud vertical fraction (UCVF), relative humidity (RH), refractory black carbon (rBC), and low cloud fraction (LCF). Circles show contributions calculated using the original normalized MLR approach, triangles show contributions based on the MLR standardized regression coefficients, and squares show SHAP-derived contributions from the standardized MLR models. Positive and negative values indicate the direction of the predictor association with the modeled response.

4. Have the authors checked whether the linear model adequately describes these relationships? Nonlinear responses and interactions are plausible, particularly for RH and cloud-related variables. A comparison with a GAM or a machine-learning model, such as random forest, would help assess the robustness of the results. I do not consider machine learning essential, but the choice of MLR should be supported by diagnostics and validation. Any alternative model should be evaluated using time-based holdouts, and its variable importance should not be treated as a chemical formation fraction.

We thank the referee for this suggestion. We agree that nonlinear responses are plausible, particularly for RH and cloud-related variables, although unlikely to be strongly supported given the limitations in the observations. We therefore evaluated a generalized additive model (GAM) using the same five predictors as the MLR (O_3, UCVF, RH, LCF, and rBC). The GAM included nonlinear additive effects without interactions and was applied to O/C and each PMF factor for the annual, seasonal, and annual CNW datasets. The GAM showed stronger agreement with the observations when evaluated using the data on which it was fitted. For the annual dataset, squared Pearson correlations between measured and

GAM-predicted values ranged from 0.63 to 0.71 and were generally higher for the seasonal fits, indicating that nonlinear relationships can improve the fit to the observations (Figure R4).

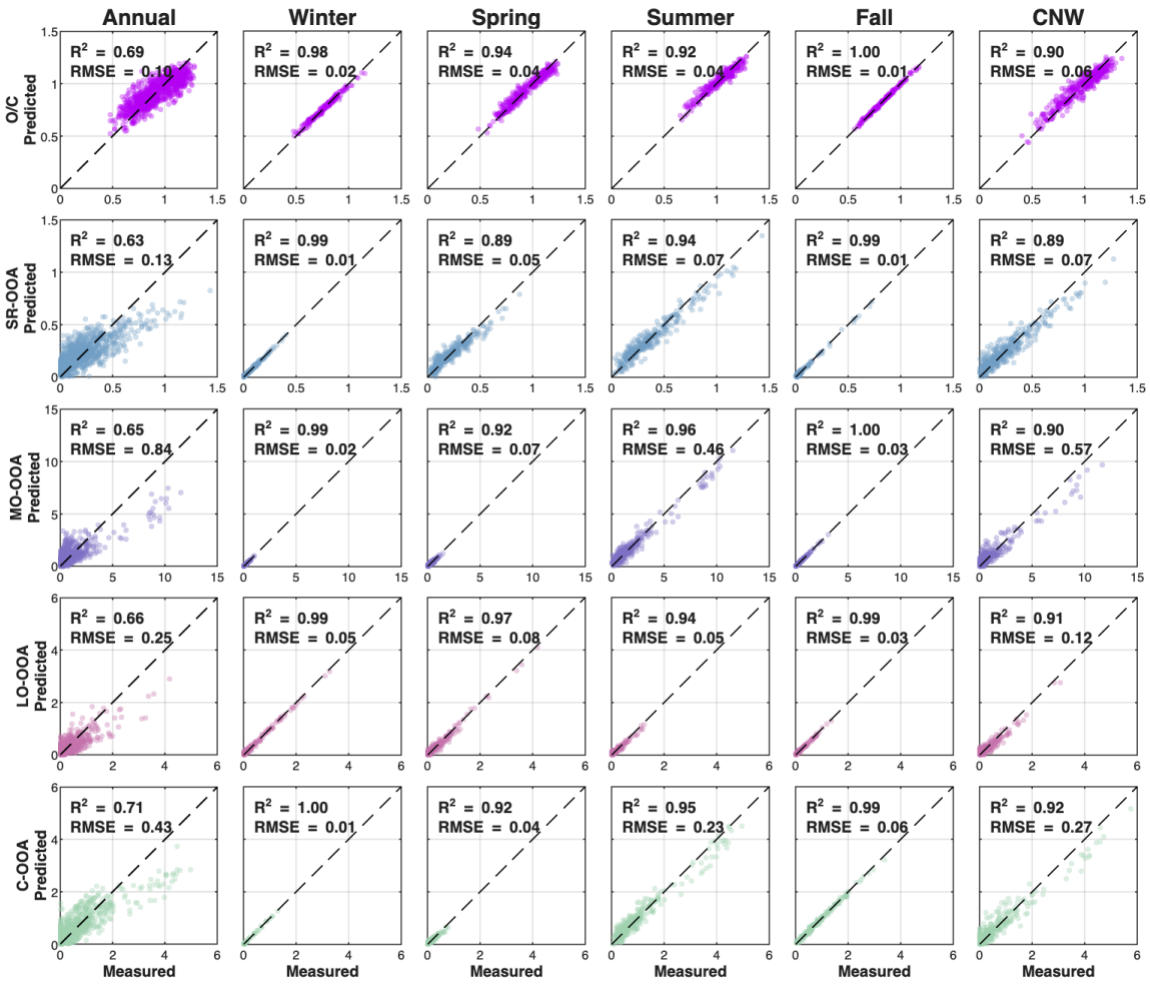


Figure R4. Predicted versus measured O/C and PMF factor mass concentrations from the generalized additive models (GAMs) for the annual, seasonal, and Coastal Northwest (CNW) datasets. Rows show O/C, SR-OOA, MO-OOA, LO-OOA, and C-OOA. The dashed line indicates the 1:1 relationship. The squared Pearson correlation coefficient (R^2) and root mean square error (RMSE) are shown for each model.

Following the referee's suggestion, we also evaluated the GAM using time-based holdouts. The data were divided into five contiguous time blocks, with each block withheld from fitting and then predicted using the remaining data. Annual held-out squared Pearson correlations (R^2) ranged from 0.002 to 0.168, substantially lower than the full-data results. Thus, although the GAM can represent additional nonlinear structure in the fitted data, this additional complexity did not result in similarly strong performance for independent time periods. We therefore retain the MLR as the primary analysis and use the GAM as a sensitivity test of whether the main relationships depend on the assumption of linearity.

We also calculated SHAP values for the GAM to quantify the relative contributions of the five predictors when nonlinear relationships were allowed (Table R3). For each predictor, the

mean absolute SHAP value was normalized by the sum of the mean absolute SHAP values across all predictors and expressed as a percentage. UCVF had the largest positive SHAP contribution to SR-OOA annually (40%) and remained important across all seasons (24–31%) and for CNW trajectories (34%). UCVF also had the largest annual SHAP contribution to O/C (38%), particularly in spring (41%) and for CNW trajectories (29%). MO-OOA showed greater seasonal variability, with UCVF having the largest SHAP contribution in spring (28%), while O_3 was the largest contributor in summer (32%) and fall (30%). LO-OOA was primarily split between O_3 and rBC seasonally, with rBC as the largest contributor in winter, summer, and fall and O_3 as the largest contributor in spring, annually, and for CNW trajectories. In contrast, rBC was consistently the largest positive contributor to C-OOA annually, for CNW trajectories, and across all seasons. Notably, although nonlinear responses were expected to be particularly important for the aqueous-related variables, allowing nonlinear relationships instead increased the relative importance of rBC compared with the MLR results.

Table R3: Generalized additive model (GAM) results showing predictor contributions for predicted PMF factor mass concentrations (SR-OOA, MO-OOA, LO-OOA, C-OOA) and bulk O/C at Mt. Soledad. Predictor variables include ozone (O_3), upwind cloud vertical fraction (UCVF), relative humidity (RH), refractory black carbon (rBC), and local cloud fraction (LCF). Relative contributions are calculated from mean absolute SHAP values relative to the five predictors, with the sign indicating whether higher predictor values are associated with higher or lower SHAP values. Results are shown for models with a fitted intercept for annual, seasonal, and CNW trajectory subsets.

Predicted Variable	Ozone	UCVF	RH	rBC	LCF
O/C					
Annual	14%	**38%**	13%	-24%	-11%
Winter	**29%**	-14%	19%	21%	17%
Spring	15%	**41%**	13%	-18%	-14%
Summer	**28%**	18%	-18%	-20%	15%
Fall	**24%**	21%	16%	-25%	14%
Annual-CNW	14%	**29%**	19%	-20%	-19%
SR-OOA					
Annual	13%	**40%**	19%	14%	-14%
Winter	18%	**24%**	-16%	-20%	23%
Spring	17%	**26%**	21%	-14%	-22%
Summer	-18%	**30%**	-16%	-15%	-20%
Fall	16%	**31%**	23%	-15%	14%
Annual-CNW	-12%	**34%**	18%	-18%	-18%
MO-OOA					
Annual	19%	15%	16%	**37%**	14%
Winter	25%	15%	-13%	**33%**	-13%
Spring	23%	**28%**	17%	17%	-16%
Summer	**32%**	-20%	14%	20%	15%
Fall	**30%**	21%	20%	18%	11%
Annual-CNW	21%	-14%	15%	**36%**	-13%
LO-OOA					
Annual	**34%**	-17%	-13%	17%	-18%
Winter	21%	22%	-18%	**24%**	-16%
Spring	**34%**	-21%	-17%	16%	-13%

Summer	23%	-19%	17%	**27%**	15%
Fall	23%	-15%	19%	**27%**	-15%
Annual-CNW	**32%**	-18%	17%	15%	-17%
C-OOA					
Annual	11%	-15%	10%	**51%**	-13%
Winter	-14%	15%	11%	**50%**	-10%
Spring	-22%	21%	-19%	**22%**	-17%
Summer	24%	-20%	13%	**28%**	14%
Fall	17%	-19%	19%	**32%**	-15%
Annual-CNW	18%	-14%	15%	**41%**	-13%

As discussed in our response to Comment 2, the percentages are interpreted as relative contributions of the selected processes to the modeled response, rather than as a partitioning of the variance explained by the model.

5. The process proxies require more cautious interpretation. RH is not equivalent to aerosol liquid water, and UCVF does not directly measure the cloud exposure of the sampled particles. Both may reflect changes in air-mass origin, precursor availability, or transport. Could aerosol liquid water be estimated from the available measurements? The authors should also discuss how excluding local in-cloud observations affects their comparison of local and upwind cloud influences.

We agree that relative humidity (RH) is not a direct measurement of aerosol liquid water. To evaluate this limitation, we calculated total aerosol liquid water content (ALWC) as the sum of inorganic and organic ALWC. Inorganic ALWC was calculated using ISORROPIA-II with measured temperature, RH, sulfate, nitrate, ammonium, and chloride as inputs. Sodium was not included because the available XRF Na data were reported as weekly measurements based on three filters collected across the two EPCAPE sites each week, with one filter from Mt. Soledad and two from Scripps Pier. These measurements therefore do not provide the site-specific, higher time resolution Na concentrations required for the Mt. Soledad ALWC calculation. We acknowledge that excluding Na may affect the calculated inorganic ALWC in this coastal environment, particularly during periods influenced by sea salt. Organic ALWC was estimated separately as $ALWC_{org} = \frac{org}{\rho_{org}} \rho_w \kappa_{org} \left(\frac{RH}{1-RH}\right)$, where *org* is the organic mass concentration, ρ_{org} is the density of organics, ρ_w is the density of water, κ_{org} represents the organic hygroscopicity, and RH is relative humidity. κ_{org} was estimated from O/C (Chang et al., 2010) rather than assuming a constant value, as this approach resulted in better agreement with hygroscopicity resolved from a cloud condensation nuclei counter at Mt. Soledad. However, this also means that calculated organic ALWC is inherently dependent on the organic aerosol properties that the MLR is intended to explain. Specifically, organic ALWC incorporates organic aerosol mass by scaling directly with organic mass concentration and O/C. For the O/C model, this introduces O/C itself into the ALWC predictor, while for the OA factor models, total organic mass includes the OA factors being predicted. Consistent with this dependence, calculated total ALWC was moderately correlated with organic aerosol mass (R = 0.67). As already reported in Table S4, organic aerosol mass is strongly correlated with MO-OOA (R = 0.90) and C-OOA (R = 0.88).

This dependence is also apparent in the ALWC sensitivity analysis (Table R4). When ALWC replaced RH, ALWC was the largest contributor to MO-OOA across all models. ALWC was also the largest contributor to C-OOA in the annual model, while rBC remained the largest contributor during winter and fall. Notably, replacing RH with ALWC did not increase the winter C-OOA model R^2. Therefore, particularly for MO-OOA and C-OOA, the large MLR contribution attributed to total ALWC cannot be separated from the dependence of the organic ALWC calculation on organic mass itself.

The seasonal behavior of LO-OOA provides further evidence of the potential influence of organic mass on the inferred ALWC contribution. Although the annual correlation between LO-OOA and total organic mass is weak (R = 0.36, Table S4), LO-OOA constituted approximately 40% of organic mass concentrations during winter. Correspondingly, winter exhibited the largest ALWC contribution to LO-OOA (57%) among the annual and seasonal models. Because organic ALWC scales directly with total organic mass, this large contribution indicates that variations in the relative abundance of individual OA factors can influence their apparent relationship with calculated ALWC. Therefore, the MLR contribution assigned to ALWC cannot be uniquely attributed to aerosol water aqueous reactions, particularly when the modeled factor constitutes a substantial fraction of the organic mass used to calculate ALWC.

We therefore retain RH in the primary MLR as an environmental indicator of conditions favorable to aerosol water associated oxidation. We emphasize that RH was used as a process proxy in the original manuscript and was not presented as a direct measurement of aerosol liquid water. Unlike calculated ALWC, RH does not incorporate the measured aerosol composition that the MLR is intended to interpret. As already summarized in Table S1 of the original manuscript, the use of RH as an indicator of aqueous reactions is well established in previous studies of OA formation and aging. Several studies have evaluated changes in MO-OOA and LO-OOA with RH as evidence of aqueous reactions(Rogers et al., 2025;Li et al., 2021;Xu et al., 2017;Xiao et al., 2021), while other studies have used calculated ALWC for similar interpretations. The use of RH as a process proxy is also consistent with Maneenoi et al. (2025), who used ambient RH as an indicator of aerosol water aqueous reactions. Therefore, based on the compositional dependence introduced by calculated ALWC and the intended use of RH as an environmental process proxy, we retain the original MLR formulation using RH.

Maneenoi et al. (2025) additionally used UCVF as an estimate of upwind cloud- time. Importantly, UCVF is calculated along the back trajectory of the sampled air mass and therefore accounts for the transport history and air mass origin of the aerosol. It is specifically intended to quantify the potential duration of upwind cloud processes prior to arrival at the measurement site, rather than simply representing regional cloudiness or air mass origin alone. As included in the original manuscript, we also performed the annual MLR separately for the Coastal Northwest (CNW) trajectory cluster to reduce variability associated with air mass origin and transport pathway. When RH was used in the MLR, the

largest contributor for each OA metric was consistent between the analysis including all trajectories and the CNW-only annual analysis, indicating that the annual relationships were not primarily driven by differences among trajectory clusters.

As stated in the manuscript, we exclude local in-cloud observations because during these periods the AMS measures cloud droplet residuals rather than interstitial aerosol. Including these observations would represent a different aerosol population from the ambient aerosol considered in the MLR analysis. However, excluding in-cloud aerosol measurements does not exclude the influence of local clouds from the analysis. Local cloud fraction is included as a predictor in the MLR to represent the influence of local cloud processes on the sampled aerosol, allowing local cloud influences to be compared with upwind cloud influences represented by UCVF.

Table R4: Multiple linear regression (MLR) results showing standardized regression coefficients and predictor contributions to predicted PMF factor mass concentrations (SR-OOA, MO-OOA, LO-OOA, C-OOA) and bulk O/C at Mt. Soledad. Predictor variables include ozone (O_3), upwind cloud vertical fraction (UCVF), aerosol liquid water content (ALWC), refractory black carbon (rBC), and local cloud fraction (LCF). Results are shown for annual, seasonal, and CNW trajectory subsets. Model performance is evaluated using squared Pearson correlation coefficients (R^2) and root mean square error (RMSE).

Predicted Variable	Ozone	UCVF	ALWC	rBC	LCF	b	R^2	RMSE
O/C								
Annual	0.01 (4%)	**0.08 (45%)**	0.06 (35%)	-0.02 (-10%)	-0.01 (-7%)	0.92	0.44	0.13
Winter	**0.05 (52%)**	0.01 (12%)	-0.01 (-7%)	0.02 (22%)	0.01 (7%)	0.77	0.17	0.12
Spring	-0.00 (-3%)	**0.09 (57%)**	0.02 (16%)	-0.03 (-20%)	-0.01 (-5%)	0.95	0.38	0.13
Summer	**0.04 (27%)**	0.02 (11%)	0.04 (27%)	-0.04 (-27%)	-0.01 (-9%)	1.04	0.34	0.11
Fall	**0.05 (32%)**	0.03 (20%)	0.03 (20%)	-0.04 (-23%)	0.01 (6%)	0.84	0.46	0.10
Annual-CNW	0.00 (2%)	**0.08 (42%)**	0.07 (37%)	-0.02 (-12%)	-0.01 (-8%)	0.97	0.37	0.15
SR-OOA								
Annual	-0.01 (-3%)	**0.09 (47%)**	0.07 (36%)	-0.01 (-7%)	-0.01 (-6%)	0.20	0.36	0.16
Winter	0.02 (23%)	-0.00 (-2%)	**0.05 (46%)**	-0.02 (-21%)	0.01 (8%)	0.08	0.49	0.06
Spring	0.01 (4%)	0.04 (20%)	**0.08 (46%)**	-0.01 (-8%)	-0.04 (-21%)	0.21	0.40	0.11
Summer	0.01 (8%)	**0.09 (59%)**	-0.00 (-1%)	-0.03 (-19%)	-0.02 (-12%)	0.36	0.18	0.22
Fall	0.01 (8%)	0.02 (15%)	**0.08 (64%)**	-0.01 (-6%)	0.01 (8%)	0.07	0.65	0.07
Annual-CNW	0.00 (1%)	**0.10 (50%)**	0.06 (28%)	-0.02 (-9%)	-0.02 (-11%)	0.25	0.32	0.18
MO-OOA								
Annual	0.15 (8%)	-0.18 (-10%)	**1.22 (69%)**	0.08 (5%)	-0.15 (-8%)	0.77	0.69	0.79
Winter	0.06 (22%)	-0.00 (-0%)	**0.08 (30%)**	0.07 (27%)	-0.06 (-22%)	0.18	0.51	0.15
Spring	0.07 (22%)	0.07 (21%)	**0.13 (40%)**	0.02 (6%)	-0.03 (-10%)	0.28	0.55	0.16
Summer	0.55 (19%)	-0.48 (-16%)	**1.54 (52%)**	0.15 (5%)	-0.24 (-8%)	1.81	0.73	1.12
Fall	0.23 (31%)	-0.05 (-7%)	**0.36 (49%)**	0.08 (11%)	0.02 (3%)	0.53	0.79	0.22
Annual-CNW	0.17 (8%)	-0.20 (-9%)	**1.56 (71%)**	0.07 (3%)	-0.22 (-10%)	0.98	0.75	0.88
LO-OOA								
Annual	**0.16 (48%)**	-0.07 (-20%)	0.06 (17%)	0.03 (9%)	-0.02 (-6%)	0.24	0.20	0.38
Winter	0.03 (4%)	-0.07 (-9%)	**0.44 (57%)**	-0.07 (-9%)	-0.16 (-21%)	0.43	0.54	0.40
Spring	**0.26 (44%)**	-0.06 (-10%)	0.10 (16%)	0.12 (19%)	-0.06 (-11%)	0.26	0.46	0.35
Summer	0.04 (19%)	-0.04 (-21%)	**0.07 (34%)**	0.05 (23%)	-0.01 (-3%)	0.13	0.27	0.19
Fall	0.09 (27%)	-0.04 (-12%)	**0.10 (30%)**	0.06 (17%)	-0.05 (-14%)	0.21	0.33	0.21
Annual-CNW	**0.14 (40%)**	-0.09 (-25%)	0.08 (22%)	0.03 (9%)	-0.02 (-4%)	0.20	0.24	0.33

C-OOA								
Annual	-0.03 (-3%)	-0.16 (-14%)	**0.56 (50%)**	0.25 (22%)	-0.13 (-11%)	0.53	0.63	0.47
Winter	0.01 (5%)	0.01 (6%)	-0.00 (-2%)	**0.17 (78%)**	-0.02 (-9%)	0.09	0.56	0.15
Spring	-0.05 (-34%)	-0.01 (-4%)	**0.05 (31%)**	0.01 (5%)	-0.04 (-26%)	0.10	0.18	0.13
Summer	0.16 (11%)	-0.26 (-19%)	**0.64 (47%)**	0.23 (17%)	-0.09 (-7%)	1.06	0.62	0.63
Fall	0.10 (10%)	-0.15 (-15%)	0.29 (29%)	**0.33 (34%)**	-0.11 (-11%)	0.88	0.49	0.47
Annual-CNW	0.03 (2%)	-0.11 (-10%)	**0.71 (63%)**	0.15 (14%)	-0.12 (-11%)	0.52	0.69	0.49

6. Please provide more information on PMF stability, including sensitivity to initialization and rotation, and whether the factor profiles remain representative across seasons. The increase in Q/Qmathrm from the two-factor to the three-factor solution in Table S2 also needs explanation. The wildfire sensitivity analysis is useful, but the resulting changes in regression contributions should be more clearly acknowledged when presenting seasonal conclusions.

We thank the referee for this comment. We have expanded the methods to include additional information on the sensitivity to rotational stability and initialization of the PMF solution:

New Lines 188–196. “The effect of rotational ambiguity was evaluated by varying fpeak from -1 to 1 in increments of 0.2. Factor mass spectra and temporal trends were largely unchanged across the tested fpeak values, indicating a stable factor solution. Differences in Q/Q_{exp} among the rotations were minimal, but fpeak = 0 was retained as it yielded the lowest Q/Q_{exp}. The stability of the solution was further evaluated using 50 random seed runs. The selected factor solution (5-factors, fpeak = 0, seed = 0) was reproduced in 32 of the 50 runs (64%). In the remaining 18 runs, two OOA factors exhibited nearly identical mass spectra (uncentered R > 0.99), indicating a non-meaningful splitting of a single OOA component. Q/Q_{exp} differed by less than 0.1% between the two solution types. The selected solution was therefore retained as the factor solution most consistently reproduced across the seed runs.”

To evaluate whether the annual PMF factors remained representative across seasons, we additionally performed PMF independently for winter, spring, summer, and fall following the method described in the manuscript. The 1 to 8 factor solutions and criteria of PMF analysis are summarized in Tables R4–R7. Seasonal solutions were evaluated, and temporal Pearson correlations (R) between the seasonal PMF factors and the corresponding annual factors were used to assess whether each factor was reproduced within a given season.

Winter: The four-factor solution reproduced SR-OOA (R = 0.70), MO-OOA (R = 0.86), LO-OOA (R = 0.98), and HOA (R = 0.99). C-OOA was not independently resolved and was instead associated with the same seasonal factor as MO-OOA (R = 0.81). This is consistent with the low winter contribution of C-OOA (median = 0.00 μg m^{-3}), which limited its independent separation within the winter subset.

Spring: The four-factor solution reproduced SR-OOA (R = 0.94), MO-OOA (R = 0.86), LO-OOA (R = 0.93), and HOA (R = 0.99). Similar to winter, C-OOA was not independently resolved as C-OOA only weakly correlated with the same factor as MO-OOA (R = 0.33), consistent with its small spring contribution (median = 0.01 μg m^{-3}). Although its correlation increased in the five-factor solution (R = 0.78), the additional factor resulted in splitting of the other factors, with none of the annual factors associated with the fifth additional factor, supporting the four-factor interpretation.

Summer: The four-factor solution reproduced SR-OOA (R = 0.96), MO-OOA (R = 0.99), HOA (R = 0.98), and C-OOA (R = 0.94). LO-OOA was not independently resolved, consistent with a lower summer contribution (median = 0.00 μg m^{-3}). Increasing to five factors did not resolve a factor that had a strong, independent correlation to LO-OOA.

Fall: In the four-factor solution, MO-OOA (R = 0.86) and HOA (R = 0.99) were strongly reproduced, while the same seasonal factor was correlated with both LO-OOA (R = 0.80) and C-OOA (R = 0.91). SR-OOA was not independently resolved, consistent with its low fall contribution (median = 0.03 μg m^{-3}). Even in the five-factor solution, its strongest temporal correlation was R = 0.44.

Overall, the seasonal PMF analysis shows that the annual factors were generally reproduced when their mass concentrations were sufficiently high within a given season, whereas factors with lower seasonal mass concentrations were either not independently resolved or merged with other OOA components. C-OOA was less clearly separated from other OOA factors within the individual seasonal subsets. The broader range of aerosol composition and source conditions represented by the annual dataset allowed the biomass-burning-related C-OOA factor to be more clearly resolved from the other OOA components.

We thank the referee for identifying the apparent increase in Q/Q_{exp} between the two- and three-factor solutions in Table S2. The Q/Q_{exp} value reported for the two-factor solution contained an error and has been corrected from 1.23 to 2.23. With this correction, Q/Q_{exp} decreases from the two-factor to the three-factor solution, as expected with increasing factor number.

We also repeated the wildfire sensitivity analysis using the revised standardized MLR. In contrast to the previous MLR analysis using min-max normalization of predictors, excluding the September 21–28 wildfire period did not increase the variability captured by the MLR. The models excluding the wildfire period instead had lower R^2 values than the corresponding models including this period. Because the previously reported improvement in model performance after wildfire exclusion was not reproduced with the revised standardized analysis, we do not highlight the wildfire sensitivity analysis in the Conclusions.

Table R5: Summary of solutions and criteria used for PMF analysis of AMS NR HR-Org during winter. Criteria that are not applicable for one factor are indicated by N/A. Paired factors that do not have uncentered correlation coefficients (UC) higher than 0.8 are indicated by None.

Factor number (p) / Criteria	1	2	3	4	5	6	7	8
Q/Q_{exp}	2.13	1.59	1.49	1.41	1.35	1.30	1.26	1.23
Absolute residual	0.35	0.29	0.27	0.25	0.25	0.19	0.19	0.19
Temporal correlation factors strength (R > 0.8)	N/A	None	None	None	None	1 pair	1 pair	2 pairs
Similarity of factor spectra (R > 0.8)	N/A	1 pair	1 pair	4 pairs	9 pairs	4 pairs	5 pairs	3 pairs
Factors with less than 10% total mass	None	None	None	None	None	2 factors	3 factors	3 factors

Table R6: Summary of solutions and criteria used for PMF analysis of AMS NR HR-Org during spring. Criteria that are not applicable for one factor are indicated by N/A. Paired factors that do not have uncentered correlation coefficients (UC) higher than 0.8 are indicated by None.

Factor number (p) / Criteria	1	2	3	4	5	6	7	8
Q/Q_{exp}	2.57	1.94	1.74	1.66	1.58	1.54	1.51	1.47
Absolute residual	0.45	0.33	0.32	0.31	0.29	0.29	0.25	0.24
Temporal correlation factors strength (R > 0.8)	N/A	None	None	None	None	1 pair	2 pair	1 pair
Similarity of factor spectra (R > 0.8)	N/A	1 pair	1 pair	3 pairs	6 pairs	7 pairs	5 pairs	5 pairs
Factors with less than 10% total mass	None	None	1 factor	1 factor	2 factors	3 factors	4 factors	5 factors

Table R7: Summary of solutions and criteria used for PMF analysis of AMS NR HR-Org during summer. Criteria that are not applicable for one factor are indicated by N/A. Paired factors that do not have uncentered correlation coefficients (UC) higher than 0.8 are indicated by None.

Factor number (p) / Criteria	1	2	3	4	5	6	7	8
Q/Q_{exp}	2.47	2.11	1.95	1.85	1.80	1.77	1.75	1.73
Absolute residual	0.54	0.43	0.41	0.39	0.36	0.34	0.33	0.33
Temporal correlation factors strength (R > 0.8)	N/A	None	None	None	None	None	1 pair	1 pair
Similarity of factor spectra (R > 0.8)	N/A	None	1 pair	2 pairs	3 pairs	6 pairs	6 pairs	7 pairs
Factors with less than 10% total mass	None	None	None	1 factor	2 factors	2 factors	3 factors	4 factors

Table R8: Summary of solutions and criteria used for PMF analysis of AMS NR HR-Org during fall. Criteria that are not applicable for one factor are indicated by N/A. Paired factors that do not have uncentered correlation coefficients (UC) higher than 0.8 are indicated by None.

Factor number (p)	1	2	3	4	5	6	7	8

Criteria								
Q/Q_{exp}	2.56	2.06	1.92	1.87	1.83	1.80	1.77	1.74
Absolute residual	0.40	0.31	0.26	0.25	0.24	0.22	0.22	0.21
Temporal correlation factors strength (R > 0.8)	N/A	None	None	None	None	None	None	1 pair
Similarity of factor spectra (R > 0.8)	N/A	None	1 pair	3 pairs	3 pairs	4 pairs	3 pairs	9 pairs
Factors with less than 10% total mass	None	None	None	None	1 factor	2 factors	3 factors	3 factors

Minor comments

7. Please check the subtraction direction used to define “OminusC” in line 170.

   We thank the referee for noting this. We have revised the text to explicitly clarify the subtraction direction used to define “OminusC”:

   New Lines 184–185. “The “OminusC” data type, obtained by subtracting the “Closed” ion sticks from the “Open” ion sticks after peak fitting, was used for PMF analysis.”

8. The C-OOA N/C value in the text differs from Table S3, and some seasonal values appear inconsistent with Table S7.

   We thank the referee for identifying these inconsistencies. We have corrected the C-OOA N/C value in the manuscript from 1.3×10^{-2} to 1.7×10^{-2} to be consistent with Table S3. We also corrected the seasonal rBC values discussed in the text, which previously referred to fall and winter, to report the summer (57 ± 62 ng m^{-3}) and fall (89 ± 152 ng m^{-3}) values consistent with Table S7:

   New Lines 439–441. “rBC increased during summer (57 ± 62 ng m^{-3}, Table S7) into fall (89 ± 152 ng m^{-3}, Table S7), showing a strong combustion influence that tracks closely with both C-OOA and HOA.”

   We have also corrected the range of the normalized difference between the maximum and minimum hourly mean concentration of C-OOA from 49–79% to 39–79% in the text.

9. Please check the duplicated captions of Figs. S6 and S9, outdated table references in Text S1, and the “Table S#” placeholder in Fig. S10.

   We thank the referee for pointing out these issues. We checked the captions for Figures S6 and S9 and found that the Figure S9 caption had been duplicated from Figure S8. The Figure S9 caption has been corrected to read: “Monthly and seasonal scatterplots of C-OOA mass concentration against rBC.” The Figure S6 caption was checked and was already correct. In Text S1, the outdated table references have been corrected from Table S16 to

Table S11, Table S17 to Table S12, and Table S9 to Table S6. We also replaced the "Table S#" placeholder in Figure S10 (now Figure S11) with "Table S8."

10. UCVF should be defined consistently as either "vertical fraction" or "volume fraction."

    We thank the referee for identifying this inconsistency. We have corrected the Table 1 caption, which incorrectly defined UCVF as "volume fraction." UCVF is now consistently defined as "vertical fraction" throughout the manuscript.

11. Please explain the weighting used to calculate O/C in Fig. S14 and report how much data were removed by the 8000 cm-3.

    The Figure S14 (now Figure S15) caption has been updated to clarify that the contributions to O/C were calculated from factor-specific O/C values weighted by the corresponding PMF factor mass concentrations: "Figure S15. Seasonal average contributions of AMS NR organic PMF factors to O/C at Mt. Soledad. Contributions were calculated from factor-specific O/C values weighted by factor mass concentrations. All measurements exclude times with particle number concentrations exceeding 8000 cm^{-3}." Specifically, for each time point, the mass fraction of each PMF factor relative to the total organic mass was multiplied by that factor's O/C, such that the resulting value represents the factor's mass-weighted contribution to the bulk O/C. These contributions were then averaged seasonally for Figure S14 (now Figure S15).

    We have also updated the Methods to report the amount of data removed by the 8,000 cm^{-3} particle concentration threshold:

    New Lines 116–118. "Aerosol and gas measurements herein exclude particle concentrations exceeding 8,000 cm^{-3} to account for short-lived contamination events, removing 2% of data at Mt. Soledad and 13% of data at Scripps Pier (Han et al., 2025)."

References

Chang, R., Slowik, J., Shantz, N., Vlasenko, A., Liggio, J., Sjostedt, S., Leaitch, W., and Abbatt, J.: The hygroscopicity parameter (κ) of ambient organic aerosol at a field site subject to biogenic and anthropogenic influences: relationship to degree of aerosol oxidation, Atmospheric Chemistry and Physics, 10, 5047-5064, 10.5194/acp-10-5047-2010, 2010.
Che, H., Segal-Rozenhaimer, M., Zhang, L., Dang, C., Zuidema, P., Dobracki, A., Sedlacek, A., Coe, H., Wu, H., Taylor, J., Zhang, X., Redemann, J., and Haywood, J.: Cloud processing and weeklong ageing affect biomass burning aerosol properties over the south-eastern Atlantic, Communications Earth & Environment, 3, 10.1038/s43247-022-00517-3, 2022.
Clemesha, R., Gershunov, A., Iacobellis, S., Williams, A., and Cayan, D.: The northward march of summer low cloudiness along the California coast, Geophysical Research Letters, 43, 1287-1295, 10.1002/2015GL067081, 2016.
Dedrick, J. L., Osawa, A., Russell, L. M., Miller, M. A., Robinson, L., Chang, R., Williams, A. S., Berta, V. Z., Ravichandran, E., Petters, M., Wheeler, M. J., Han, S., Pelayo, C. N., Maneenoi, N., Lubin, D., Uin, J., Enekwizu, O., Zawadowicz, M., Mayol-Bracero, O., and Twohy, C. H.: Quantitative Estimates of Upwind and On-Site Particle Scavenging and Retrieved Cloud

Supersaturations from Urban Coastal Stratocumulus during EPCAPE, Journal of the Atmospheric Sciences, 83, 1061-1082, https://doi.org/10.1175/JAS-D-26-0004.1, 2026.
Dobracki, A., Lewis, E., Sedlacek, A. I., Tatro, T., Zawadowicz, M., and Zuidema, P.: Burning conditions and transportation pathways determine biomass-burning aerosol properties in the Ascension Island marine boundary layer, Atmospheric Chemistry and Physics, 25, 2333-2363, 10.5194/acp-25-2333-2025, 2025.
Dong, Z., Li, X., Su, F., Kong, Z., Shang, L., Li, Z., and Zhang, R.: Molecular-scale investigation on the composition, sources and secondary generation of organic aerosols in polluted central China, JOURNAL OF CLEANER PRODUCTION, 434, 10.1016/j.jclepro.2023.139830, 2024.
Han, S., S., W. A., M., R. L., Z., B. V., L., D. J., Christian, P., Nattamon, M., Atsushi, O., Israel, S., Damao, Z., A., Z. M., and Sedlacek Arthur J., I.: Nearby Sites Show Similar Upwind Sources and Differing Semivolatile Concentrations in Coastal Aerosol Particles, ACS EST Air, 2, 2824-2837, 10.1021/acsestair.5c00191, 2025.
Heutte, B., Angot, H., Chen, G., Pernov, J., El Haddad, I., Dada, L., Daellenbach, K., Beck, I., Bergner, N., Bucci, S., Creamean, J., Kulmala, M., Laurila, T., Petaja, T., Pratt, K., Prevot, A., Quelever, L., Zieger, P., Jokinen, T., and Schmale, J.: Sources and Composition of Organic Aerosols in the Central Arctic during Spring and Summer, Environmental Science & Technology, 59, 21924-21940, 10.1021/acs.est.5c09788, 2025.
Hoppel, W., Fitzgerald, J., Frick, G., Larson, R., and Mack, E.: Aerosol Size Distributions and Optical-Properties Found in the Marine Boundary-Layer over the Atlantic-Ocean, Journal of Geophysical Research-Atmospheres, 95, 3659-3686, 10.1029/JD095iD04p03659, 1990.
Li, J., Cao, L., Gao, W., He, L., Yan, Y., He, Y., Pan, Y., Ji, D., Liu, Z., and Wang, Y.: Seasonal variations in the highly time-resolved aerosol composition, sources and chemical processes of background submicron particles in the North China Plain, Atmospheric Chemistry and Physics, 21, 4521-4539, 10.5194/acp-21-4521-2021, 2021.
Liu, S., Day, D. A., Shields, J. E., and Russell, L. M.: Ozone-driven daytime formation of secondary organic aerosol containing carboxylic acid groups and alkane groups, Atmospheric Chemistry and Physics, 11, 8321-8341, 10.5194/acp-11-8321-2011, 2011.
Maneenoi, N., Russell, L. M., Han, S., Dedrick, J. L., Williams, A. S., Berta, V. Z., Pelayo, C., Zawadowicz, M. A., Sedlacek, A. J., 3rd, Silber, I., Thieman, M., Painemal, D., and Shen, S. S. P.: Photochemical and Cloud and Aerosol Aqueous Contributions to Regionally-Emitted Shipping and Biogenic Non-Sea-Salt Sulfate Aerosol in Coastal California, ACS EST Air, 2, 648-664, 10.1021/acsestair.4c00352, 2025.
Maria, S. F., Russell, L. M., Gilles, M. K., and Myneni, S. C. B.: Organic aerosol growth mechanisms and their climate-forcing implications, Science, 306, 1921-1924, 10.1126/science.1103491, 2004.
Parrish, D., Galbally, I., Lamarque, J., Naik, V., Horowitz, L., Shindell, D., Oltmans, S., Derwent, R., Tanimoto, H., Labuschagne, C., and Cupeiro, M.: Seasonal cycles of O3 in the marine boundary layer: Observation and model simulation comparisons, Journal of Geophysical Research Letters-Atmospheres, 121, 538-557, 10.1002/2015JD024101, 2016.
Rogers, M., Joo, T., Hass-Mitchell, T., Canagaratna, M., Campuzano-Jost, P., Sueper, D., Tran, M., Machesky, J., Roscioli, J., Jimenez, J., Krechmer, J., Lambe, A., Nault, B., and Gentner, D.: Humid Summers Promote Urban Aqueous-Phase Production of Oxygenated Organic Aerosol in the Northeastern United States, Geophysical Research Letters, 52, 10.1029/2024GL112005, 2025.
Xiao, Y., Hu, M., Zong, T., Wu, Z., Tan, T., Zhang, Z., Fang, X., Chen, S., and Guo, S.: Insights into aqueous-phase and photochemical formation of secondary organic aerosol in the winter of Beijing, Atmospheric Environment, 259, 10.1016/j.atmosenv.2021.118535, 2021.
Xu, W., Han, T., Du, W., Wang, Q., Chen, C., Zhao, J., Zhang, Y., Li, J., Fu, P., Wang, Z., Worsnop, D., and Sun, Y.: Effects of Aqueous-Phase and Photochemical Processing on

Secondary Organic Aerosol Formation and Evolution in Beijing, China, Environmental Science & Technology, 51, 762-770, 10.1021/acs.est.6b04498, 2017.